Manufacturing Rev. **4**, 8 (2017)

DOI: 10.1051/mfreview/2017010

Manufacturing Review
Available online at:
http://mfr.edp-open.org

RESEARCH ARTICLE OPEN ACCESS

FE modeling of a complete warm-bending process for optimal design of heating stages for the forming of large-diameter thin-walled Ti–6Al–4V tubes

Zhijun Tao[1], Heng Li[1,*], Jun Ma[1], Heng Yang[1], Chao Lei[1], and Guangjun Li[2]

[1] State Key Laboratory of Solidification Processing, School of Materials Science and Engineering, Northwestern Polytechnical University, Xi'an 710072, P.R. China
[2] Chengdu Aircraft Industry (Group) Corporation Ltd., Chengdu 610092, P.R. China

Received: 8 June 2017 / Accepted: 30 June 2017

Abstract. Warm rotary draw bending (WRDB) of large-diameter thin-walled (LDTW) Ti–6Al–4V tube is a multi-nonlinear thermo-mechanical coupled process. Due to the high-cost, energy-wasting and long-term, the traditional physical experiments based on "trial and error" are no longer suitable for the WRBD process. Considering the non-uniform local heating and multi-tool constraints, a thermal–mechanical coupled 3D FE model of complete WRDB process for LDTW Ti–6Al–4V tube is established on ABAQUS as heating-bending-unloading three-stage. The FE models could predict the overall temperature distribution, describe thermo-mechanical bending deformation considering a modified Johnson–Cook model, and simulate the heating-bending-springback-cooling process. On that basis, the temperature distributions on both tube and dies under various heating schemes are compared, and the optimal heating scheme is determined on the basis of forming quality and efficiency. Combined with the experiments of WRDB, the optimal heating scheme and the established FE models are verified. In conclusion, the FE simulation provides a replacement of physical experiment and a convenient method of deformation prediction for WRDB of LDTW Ti–6Al–4V tube.

Keywords: warm rotary draw bending (WRDB) / complete process / FE modeling / heating scheme / parameter optimization / LDTW Ti–6Al–4V tube

1 Introduction

As one typical kind of light-weight and high-performance components, large-diameter thin-walled (LDTW) Ti–6Al–4V bent tubes are urgently needed in many industries such as aviation, aerospace, automobile and energy [1–4]. Rotary draw bending, due to its advantages in achieving high-quality products and stable bending process, has become an ideal approach for manufacturing LDTW titanium tubes. However, constrained by the limited formability of LDTW Ti–6Al–4V tube, cracking and wrinkling are the incredible problems during cold bending [5–8]. Warm-bending (room temperature $< T_w <$ recrystallization temperature) may be a feasible way for manufacturing these components [9,10].

Warm rotary draw bending (WRDB) of Ti–6Al–4V tube is a complex thermo-mechanical coupled plastic forming process with multi-tool constraints and multi-factor interacted effects. Among them, temperature fields is one of the most important issue affecting the material properties and bending process, which directly determines whether the Ti–6Al–4V bent tubular parts can be achieved or not. Increasing working temperature leads to the reduction of deformation resistance and the improvement of formability in many metal forming processes, such as aluminum, magnesium and commercial pure titanium. With the increase of temperature, the decreased flow stress reduces the deformation resistance of Ti–6Al–4V tube, which is helpful for the flow of the tube material. For example, the flow stress has an obvious drop of about 50% at temperature increasing to 873 K [9]. However, the elevated temperatures also strengthen the constraint effects of the bending dies. Meanwhile, different heating strategies of each bending dies will result in the different temperature distribution on Ti–6Al–4V tube, which has a significant effect on the non-uniform temperature controlled warm-bending process. As a result, the coupling effects of thermal and mechanical parameters make the bending deformation even more complex. Therefore, it is

* e-mail: liheng@nwpu.edu.cn

urgent to investigate the temperature related bendability of WRDB for Ti–6Al–4V tube to prevent the possible defects, and the effect of reasonable temperature distribution on forming properties to improve the bending quality.

To date, numerous efforts have been conducted to investigate the deformation behaviors and formability of titanium sheets and bars at elevated temperatures. Kotkunde et al. [11] proposed a set of isothermal uniaxial tests of Ti–6Al–4V flat-sheet samples at temperature range from room temperature up to 650 °C, and noticed the complicated interaction between strain hardening and thermal effects. Compared with room temperature condition, approximately half the ultimate tensile stress and twice the maximum strain of Ti–6Al–4V are achieved at 650 °C, as proved by Lai et al. [12]. Chen et al. [13] studied the temperature dependent work hardening in Ti–6Al–4V alloy over large temperature range (20–900 °C). Therefore, it can be seen that bending at elevated temperature can be carried out to form LDTW Ti–6Al–4V bent tubes. Wu et al. [14] found that heating could improve the bending ability of wrought magnesium alloy AM30 tubes using a rotary draw bender at 473 K and bending velocity of 8 mm/s. Luo et al. [15] also proved that it was feasible to bend magnesium alloy AZ31 tubes at elevated temperature (423–473 K). Jin et al. [16] showed the deformation mechanisms of magnesium tube bending at elevated temperature. Zhang et al. [17] studied the quasi-static tensile behavior of LDTW CP-Ti tubes at various temperature ranges and different strain rates, and achieved that the optimal temperature for tube warm-bending is 573 K. All of above studies have laid the groundwork for Ti–6Al–4V tube warm-bending.

However, WRDB of LDTW Ti–6Al–4V tube is a highly nonlinear unstable forming process including multiple constraints and complex thermal–mechanical coupling effects, which is quite difficultly studied and needs large cost consuming by using experimental. In the last two decades, FE simulation has become an increasing important tool for investigating metal forming processes [18–20]. FE simulation can provide convenience not only to make clear the forming mechanisms, temperature effects, traces of deformation, microstructure evolutions and an insight into how defects arise during the forming process, but also to give an efficient method to identify and optimize important process parameters without expensive experiments [21–24]. Therefore, it's important to develop a reasonable FE model for the investigation and understanding of tube warm-bending, which should be as consistent with the real conditions as possible and can save computation time.

Many scholars have studied the tube bending by combining the FE method with the experimental and analytical methods, especially applied to aluminum alloy tube and stainless steel tube [25–29]. Reliable FE models of cold tube bending were established so as to analyze stress and strain distribution, predict instability wrinkling behavior, solve springback problem, optimize process parameters and obtain qualified bent tube. Jiang et al. [30,31] established bending-springback FE model of titanium tube cold bending. Trana [32] studied the bending process of high strength steel tube by combining FE simulation and experiment. Till now, the FE simulation method has been applied on various tube heating bending processes. Zhang et al. [33] provide useful knowledge for the FE modeling of warm-bending and the realization of the precision bending of LDTW CP-Ti tubes. Hu et al. [34,35] established a local induction heat bending model of steel tube with small bending radius. Zhou et al. [36] established a hot push bending model of TA2 ring pipe. Li et al. [37] simulated a medium frequency induction heating bending process of pure titanium tube. Dai et al. [38] simulated a hot push bending process of Ti–6Al–4V tube. The above studies lay the foundation and prove the feasibility of Ti–6Al–4V tube warm-bending.

To further study the forming rules of WRDB and achieve excellent bent tube of Ti–6Al–4V alloy, this paper proposed a complete process model of heating-bending-unloading, and then focused on the optimal design of heating system to achieve the reasonable temperature distribution. Then, the FE model of warm-bending is established and used to predict wall thinning, wrinkling and cross-section distortion and even fracture. The optimal heating method could establish a sound preliminary thermal condition to improve heat bending formability and reduce energy consumption.

2 FE modeling of complete warm-bending process

2.1 Characteristics of WRDB for Ti–6Al–4V tube

In order to obtain precision LDTW Ti–6Al–4V bent tubes, a group of heating resistors is applied on different parts of the die system to make tubes be heated to required temperature of warm-bending. Then the tube is clamped by clamp die and bend die to finish rotary draw bending with the helpful push of pressure die. Finally, all of the dies unload after the bending angle satisfied the request, and then the bent tube will springback. However, due to the original defect, the performance of Ti–6Al–4V tube is nonlinearity. The bending process is operated by multi-dies which will lead to non-linearity of contacts and boundary conditions. The uneven deformation of Ti–6Al–4V tube leads to complex geometrical nonlinearity. The coupling of the temperature field and the stress field in the process of deformation makes the bending deformation more complicated. As a result, under the superimposed effect of uneven temperature field and stress field, tube warm-bending is extremely complex (Fig. 1). If the forming parameters are not properly chosen, instability of bending process such as wrinkling, cross section distortion and fracture, will occur and get out of hand.

The warm-bending experiments are performed at different temperatures with improved W27YPC-159 tube bending equipment made mainly by 45# steel. The experimental Ti–6Al–4V tubes with the nominal outer diameter (OD) of 60 mm and the nominal thickness of 1 mm ($D60 \times t1$ mm). Figure 2a shows the principle of warm-bending process and Figure 2b shows 3D solid modeling drawing of bending dies.

A set of designed bending dies has been developed to match the W27YPC-159 bending machine for warm-bending. The dies of warm-bending are composed

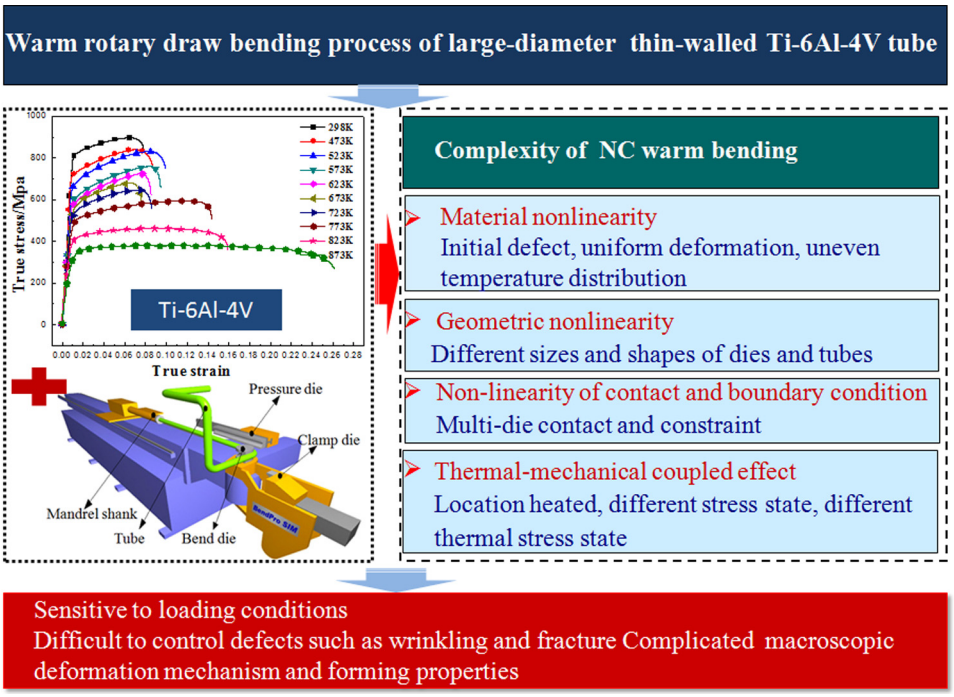

Fig. 1. Characteristics of warm bending for Ti–6Al–4V tube.

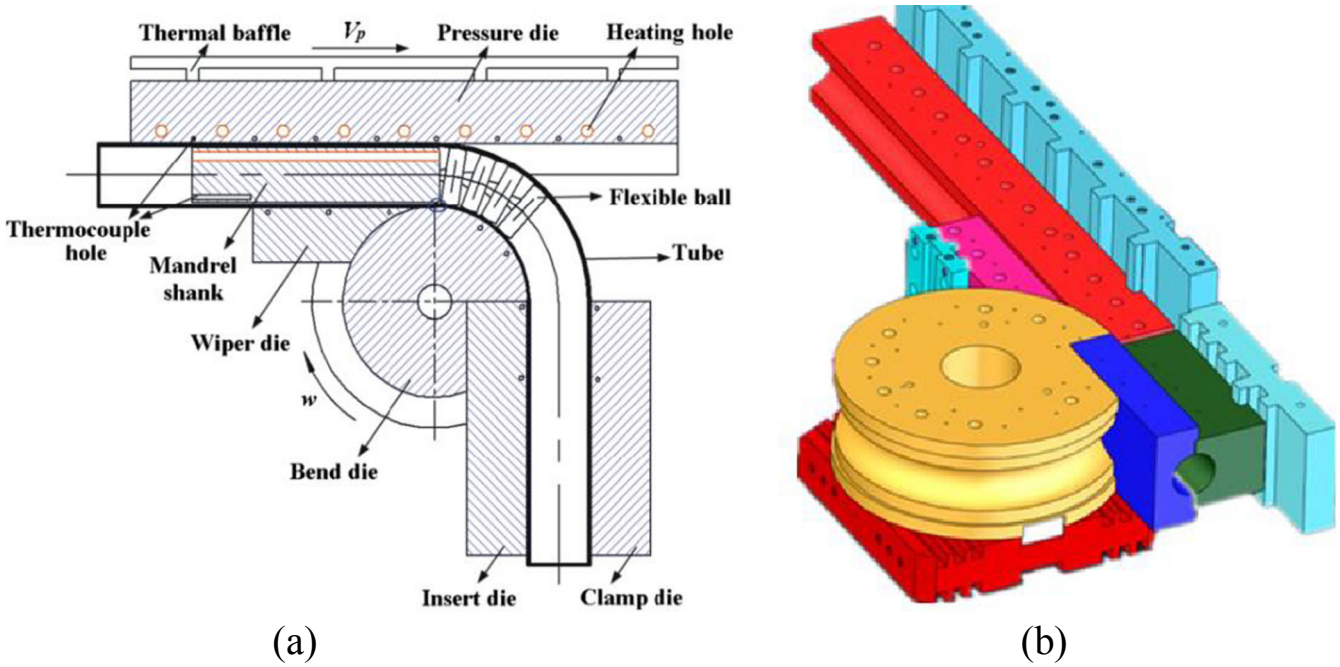

Fig. 2. Process principle [33] (a) and 3D solid modeling (b) of bending dies for warm bending of Ti–6Al–4V tube.

of bend die, clamp die, pressure die, wiper die and mandrel die. Considering the need of heat insulation between dies and machine to protect equipment, cooling system is needed and composed of heat shields on four parts as shown in Figure 3. The pressure die, wiper die, mandrel die and clamp die are made of H13 steel with better resistance to heat, abrasion, impact, oxidation, and erosion. All of the heat shields and bending accessories are made of 35CrMo.

2.2 Thermo-mechanical coupled 3D FE modeling of warm-bending

The thermo-mechanical 3D FE simulation for warm-bending is a three-stage process of heating-bending-unloading. In accordance with the multi-dies constraints and uneven temperature distribution of warm-bending of LDTW Ti–6Al–4V tube, the thermo-mechanical 3D FE model is developed on the FE platform of ABAQUS.

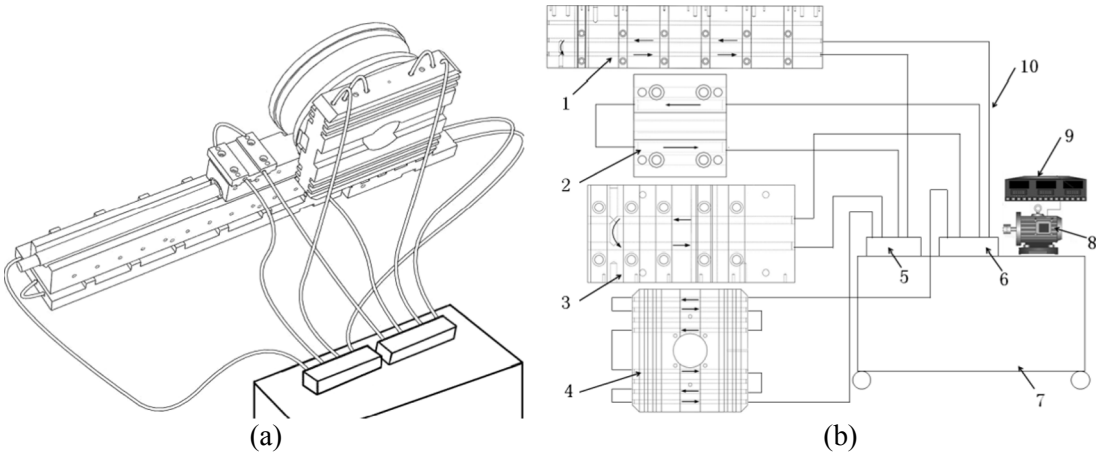

Fig. 3. Cooling system for warm bending of Ti–6Al–4V tube: (a) assembly drawing and (b) constituent parts (1 – heat shield of pressure die, 2 – heat shield of wiper die, 3 – heat shield of clamp die, 4 – heat shield of bend die, 5 – water outlet port, 6 – water inlet port, 7 – water tank, 8 – electrical power machine, 9 – controller, 10 – water pipe).

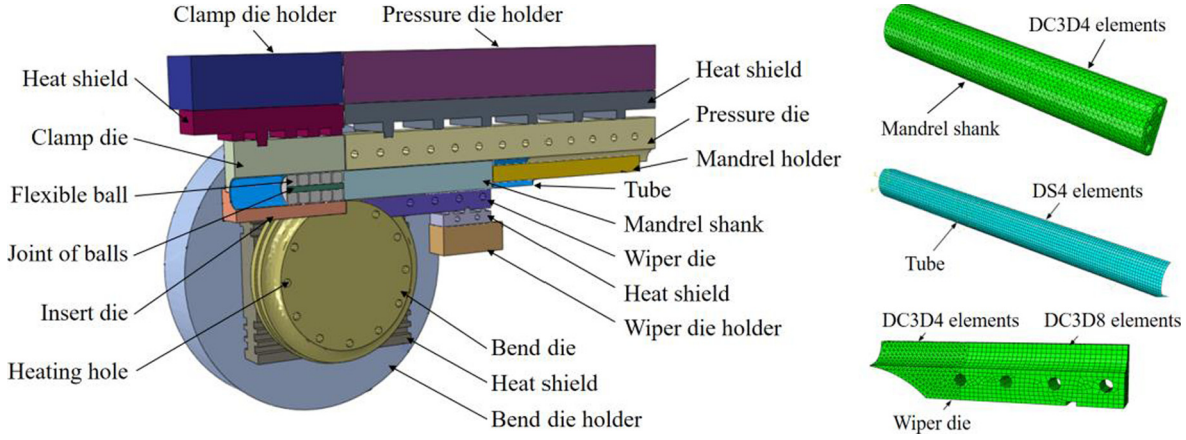

Fig. 4. 3D-FE geometric model and mesh partition for heating stage.

Table 1. Grid size at different locations of FE geometric model during heating stage.

Location	Tube, mandrel shank, flexible ball	Bend die holder	Joint of flexible ball	Other dies
Grid size (mm^2)	5×5	15×15	3×3	10×10

2.2.1 Key techniques for 3D FE modeling of heating stage

The heating stage of warm-bending of LDTW Ti–6Al–4V tube is a static heat transfer process, so the ABAQUS/Standard module is employed to discretize the geometric model into heat conduction unit with heat-transfer analysis step option. As the same time, the transient analysis step is used for the heating stage that is time-dependent.

As the large-size factor ($D/t = 60$), the Ti–6Al–4V tube is established as deformable shell body. In order to realize sufficient heating transfer between dies and tube, the FE geometric models of dies are made of 3D solid body. Due to the symmetry of Ti–6Al–4V tube, the semi-tube model is modeled to reduce the computation time. Figure 4 shows the complete 3D FE geometric model and the mesh partitions of tube, mandrel and wiper die. The four-node heat transfer quadrilateral shell element (DS4) is used to describe the Ti–6Al–4V tube, and the four node linear heat transfer tetrahedron element (DC3D4) is selected to describe the mandrel. To reduce the element quantity and computation time, the wiper die is partitioned by DC3D4 near bend die and DC3D8 (eight-node linear heat transfer brick element) at back-end. The other parts of dies are all meshed by DC3D8 elements to increase calculation efficiency. In order to balance efficiency and accuracy, a refined element is introduced in the bending deformation area of the tube, and the line segment of the bent tube is divided by the coarser

Table 2. Thermophysical property of Ti–6Al–4V.

Material	Temperature, T (°C)	Density, ρ (kg/m^3)	Coefficient of thermal conductivity, k_c (W/(m·°C))	Specific heat capacity, c (J/(kg·°C))
Ti–6Al–4V	20	4440	6.8	611
	100		7.4	624
	200		8.7	653
	300		9.8	674
	400		10.3	691
	500		11.8	703

Table 3. Interfacial heat transfer coefficient of each part.

Contact surface	Interfacial heat transfer coefficient, k (kW/(m^2·°C))
Die-tube	2.1
Bend die-insert die	2.1
Wiper die-bend die	0.7
Mandrel shank-mandrel holder	4
Flexible ball-joint of flexible ball	4
Dies-heat shield	2.5
Heat shield-machine tool	0.7

grid. Grid size at different locations of FE geometric model during heating stage is shown in Table 1. Table 2 shows the material thermal property of Ti–6Al–4V alloy.

When determining the boundary conditions, the theoretical heat transfer coefficient is inapplicable because of the existence of clearance between tube and die, which may be filled by lubricating oil and oxide skin. Therefore, the thermal conductivity of the interface is achieved by real-contacting heat transfer and heat radiation. By reason that the heat-transfer mechanism is complex, the interstitial heat transfer coefficient can be probably obtained by equation (1), where α_1 and α_2 are the heat transfer coefficient of two surfaces, λ is the heat transfer coefficient of clearance, and δ is the thickness of the clearance. Table 3 shows heat transfer coefficients between different parts. During simulation of complete process, the coefficients of heat convective are set as 20 W/(m$^2\cdot$°C) in bending process and 1000 W/(m$^2\cdot$°C) in cooling process, and the coefficient of heat emissivity is set as 0.6 W/(m$^2\cdot$°C). The thermal load definition and heating control method are referred to the stepwise inverse method for thermal conductivity of the interface determination at different contact pairs [33]. Figure 5 shows the simulation of heating stage during warm-bending process by the established model.

$$k = \frac{1}{\frac{1}{\alpha_1} + \frac{\delta}{\lambda} + \frac{1}{\alpha_2}}. \quad (1)$$

2.2.2 Key techniques for 3D FE modeling of bending stage

In order to improve the calculation efficiency of the FE model, the die geometry surface contacting directly with the tube is used to describe the various dies. Pressure die, bend die, clamp die, wiper die and mandrel die are simplified as rigid body. The tube and dies are half modeled as the reason that the symmetry is with respect to the central bending plane, and the tube is discretized by the coupled temperature–displacement shell elements S4RT (Fig. 6). At the same time, a refined mesh (Tab. 4) is used in the bending area of the tube (Fig. 6) to ensure numerical accuracy.

An accurate prediction of flow behaviors of Ti–6Al–4V considering the combined effects of strain, strain rate and temperature is essential for understanding flow responses in tube warm-bending process. Deformation behaviors and constitutive analyses of LDTW Ti–6Al–4V tube during warm-bending were investigated via quasi-static tensile tests within wide ranges of temperatures and strain rates (25–600 °C and 0.00067–0.1/s) [9,10]. A modified Johnson–Cook model [39] has been proposed by introducing nonlinear strain rate hardening and the interaction between strain hardening and thermal softening. Applied to the bending simulation, the present model exhibits good ability to capture the deformation behaviors of LDTW Ti–6Al–4V tube over the entire temperature and strain rate ranges, by successfully predicting the experimental observed defects such as over-thinning, wrinkling and fracture.

$$\sigma = (A+B\varepsilon^n)\left(1+C_1\ln\frac{\dot{\varepsilon}}{\dot{\varepsilon}_0}+C_2\left(\ln\frac{\dot{\varepsilon}}{\dot{\varepsilon}_0}\right)^2\right)(1-f_{(\varepsilon,T^*)}), \quad (2)$$

with

$$\begin{cases} f_{(\varepsilon,T^*)} = T^{*a+bT^*+cT^{*2}+dT^{*3}+eT^{*4}} \\ a = a_1+b_1\varepsilon+c_1\varepsilon^2+d_1\varepsilon^3+e_1\varepsilon^4 \\ b = a_2+b_2\varepsilon+c_2\varepsilon^2+d_2\varepsilon^3+e_2\varepsilon^4 \\ c = a_3+b_3\varepsilon+c_3\varepsilon^2+d_3\varepsilon^3+e_3\varepsilon^4 \\ d = a_4+b_4\varepsilon+c_4\varepsilon^2+d_4\varepsilon^3+e_4\varepsilon^4 \\ e = a_5+b_5\varepsilon+c_5\varepsilon^2+d_5\varepsilon^3+e_5\varepsilon^4 \end{cases}, \quad (3)$$

where a_i, b_i, c_i, d_i and e_i ($i = 1$, 2, 3, 4 and 5) are regression coefficients needed to be solved.

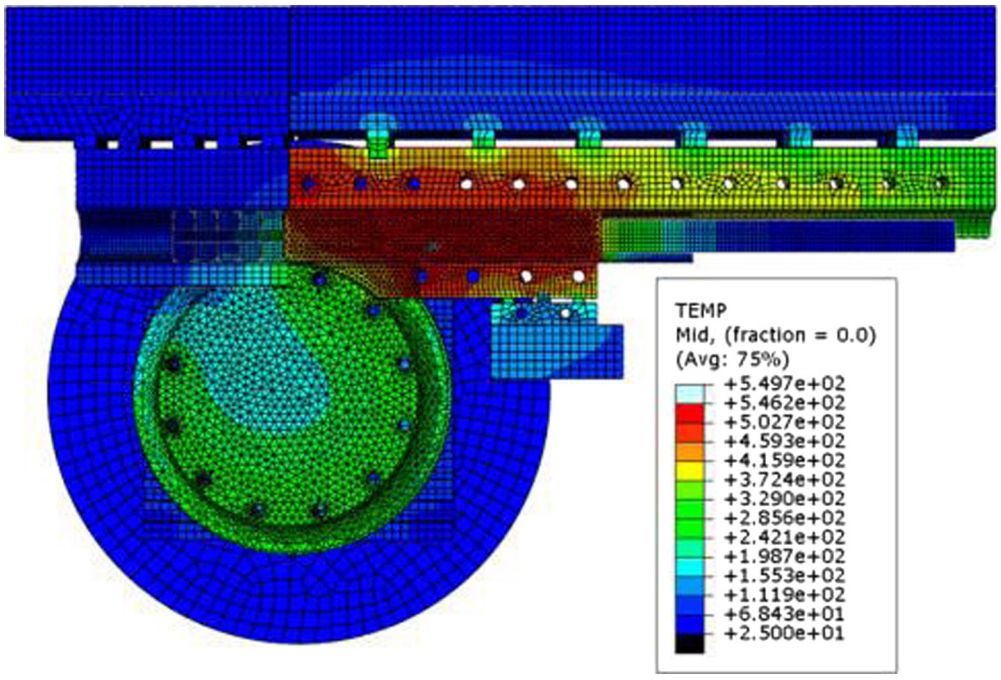

Fig. 5. Simulation of heating stage during LDTW Ti–6Al–4V tube warm bending process.

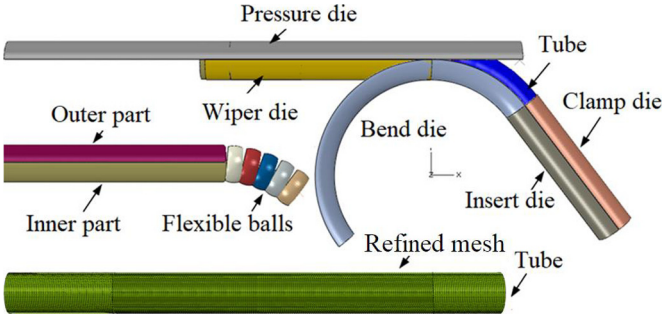

Fig. 6. FE geometric model of half tube and dies and mesh partition of tube.

The high-temperature twist compression test (TCT) was used for the determination of the tribological characteristics and the friction coefficient under various tribological conditions. Since several variables such as tube material, die material, temperature, pressure force, types of lubricant and large rotate speed can be varied under dynamic contact conditions while remaining a constant contact area in the test, the high-temperature TCT is proper to reproduce the dynamic contact conditions of warm-bending of Ti–6Al–4V tube [40,41]. Based on this research, the friction coefficients of different contact interface are defined, as shown in Table 5.

The thermal–mechanical coupling model for the warm-bending process of Ti–6Al–4V tube is consists of three steps: preheating, bending and pumping. The preheating step allows the tube to reach the designed temperature, and generate thermal expansion, while thermal expansion coefficient of Ti–6Al–4V tube is 1×10^{-5}/°C below 600 °C. Then, the bending step makes the Ti–6Al–4V tube deformed. Finally, the pumping step realizes mandrel back off.

Table 4. Grid size at different locations of the FE geometric model during bending stage.

Location	Curly segment of tube	Line segment of tube	Die
Grid size (mm^2)	1.5×1.5	2.5×2.5	2.5×2.5

Using two ways of displacement/rotation and velocity/angular to realize the contact boundary constraint and load applied, the moving mode of dies is the same with the actual tube bending process. The loading curves of the bend and pressure dies are defined by using the staircase curve to avoid the dynamic inertia effect. The bend die and the clamp die are defined as the same freedom degree, only opening the rotational freedom around the bend die center. The pressure die is only opened in the X direction. The freedom of the wiper die is restrained totally during the bending stage. The freedom of mandrel flexible balls is opened in the rotational Z direction. Figure 7 shows the load-step curve. Finally, the simulation of bending stage during warm-bending process of the LDTW Ti–6Al–4V tube is achieved (Fig. 8).

2.2.3 Key techniques for 3D FE modeling of unloading stage

When building an unloading model, the data transmit between different analysis processes is necessary. A new model should be established for import the results of previous heating and bending stages. The new model carries on the already defined element and material message. The calculation deformation step of unloading

Table 5. Parameters of tube-die surface contact.

Contact surface	Contact function	Sliding mode	Friction coefficient	Interstitial heat conduction coefficient (kW/(m^2·°C))
Tube-flexible ball	Penalty	Finite	0.1	
Tube-insert die	Kinematic	Small	Rough	
Tube-bend die	Kinematic	Finite	0.4	
Tube-clamp die	Kinematic	Small	Rough	2.1
Tube-mandrel shank	Penalty	Finite	0.1	
Tube-pressure die	Kinematic	Finite	0.4	
Tube-wiper die	Kinematic	Finite	0.1	

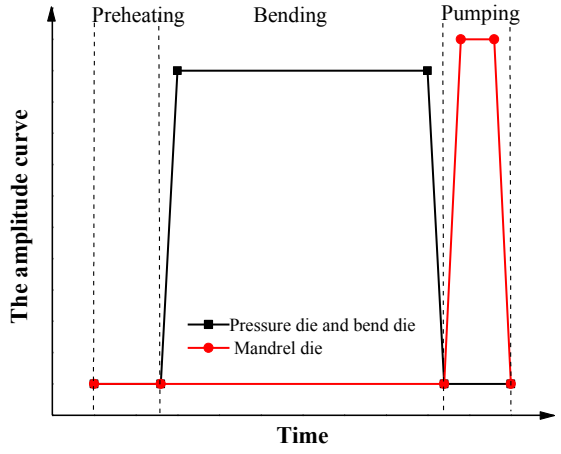

Fig. 7. Amplitude curve of pressure die, bend die and mandrel die.

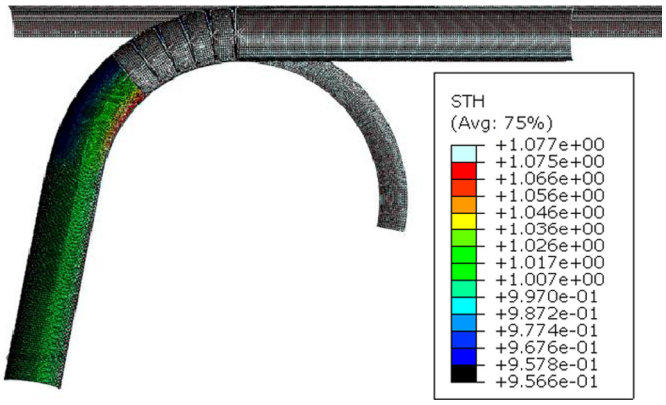

Fig. 8. Simulation of bending stage during LDTW Ti–6Al–4V tube warm bending process.

springback is identified as static/general. The Nlgeom should be set as "On" due to the springback induced large displacement. To achieve convergence of the model, dissipated energy fraction is system default, specify damping factor is 0.0002, initial increment size is 0.01, max increment size is 1 and min is 1×10^{-5}. The freedom degree of translational direction and rotation direction should be released to achieve the tube's freely deformation. Because of half-tube modeling, it's necessary to impose boundary conditions on the tube's symmetric surface. In cooling process, room temperature is 25 °C and the coefficient of heat transfer is 0.02 W/(m^2·°C). The final unloading and cooling model is shown in Figure 9.

2.3 Evaluation of the heating-bending-unloading model

The quality amplification is conducted to improve the efficiency in thermal-mechanical coupling FE model of warm-bending for Ti–6Al–4V tube. When the quality amplification factor is set as 10 000, the value of ALLKE/ALLIE rises to more than 10% at the beginning of loading time and drops back quickly, with no significant dynamic effects being introduced. The curve of ALLAE/ALLIE also shows that the hourglass in the model is lighter (Fig. 10).

3 FE-based optimal design of heating scheme

Given the complexity of warm-bending of Ti–6Al–4V tube, the tube temperature during the bending stage must be guaranteed by die temperature. In the warm-bending process, the tube is not heated directly, but its heating is implemented by heat conduction and heat radiation from heated dies. In order to guarantee the clamping strength during the bending stage, the clamp die and insert die cannot be heated. Conversely, the pressure die, bend die, wiper die and mandrel can be heated. Sometimes, the working temperature maybe up to 600 °C, thus the heat insulation board and water cooling structure are needed to prevent undesired heat transfer for protecting bending machine. The temperature distribution of dies will be influenced by different heating combinations, which will affect the bending and forming quality of Ti–6Al–4V tubes. Therefore, it is necessary to optimize the heating stage to reduce the energy consumption and ensure the reasonable temperature distribution. The study mainly focuses on heating stage and simulates the temperature distribution under different heating combination of different dies to obtain the reasonable heating scheme.

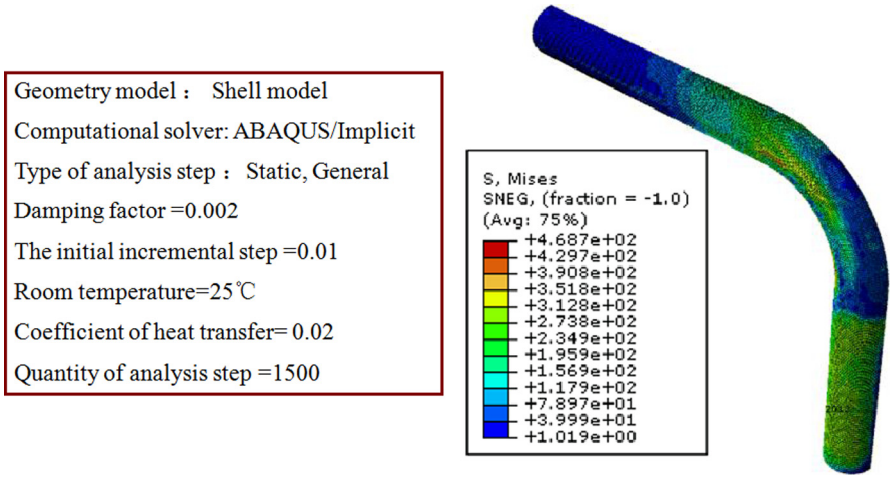

Fig. 9. Parameter setting and simulation of unloading stage during LDTW Ti–6Al–4V tube warm bending process.

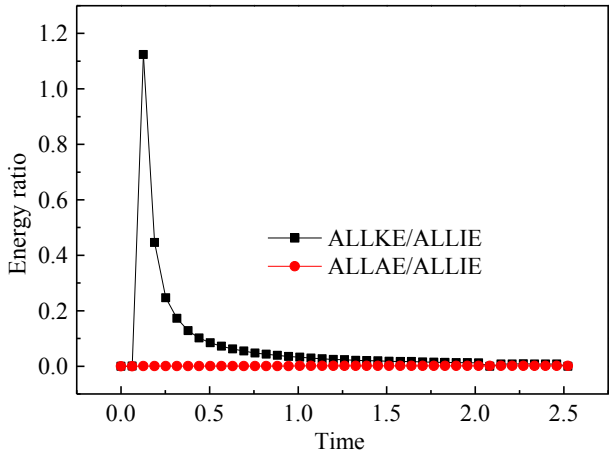

Fig. 10. Value of ALLKE/ALLIE and ALLAE/ALLIE.

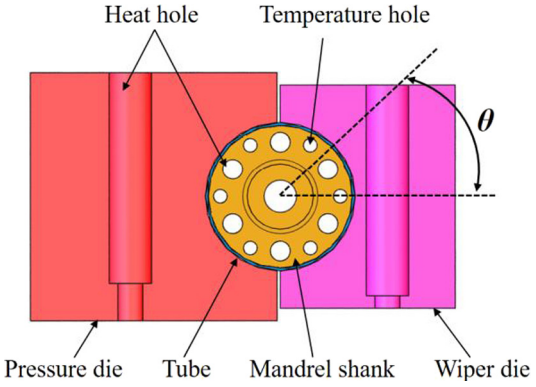

Fig. 11. Definition of θ.

3.1 Determination of heating schemes

During the heating stage, the highest temperature position must be the point where the elongation of the tube is the largest. The heating location should be nearby the inside surface of the tube and the outside surface of the dies, which can maintain bending temperature and increase heating efficiency. In consequence, the pressure die, mandrel die, bend die and wiper die must be heated. However, the large volume of bend die leads to severe heat consumption, resulting in difficulty for heating to the desired temperature. To achieve even temperature distribution, six combination schemes of heating system are proposed:

- the 1st heating scheme: heating the pressure die and mandrel die;
- the 2nd heating scheme: heating the pressure die, wiper die and mandrel die;
- the 3rd heating scheme: heating the pressure die, wiper die, mandrel die and bend die, and at the same time, cooling the heat shields nearby the pressure die, wiper die and bend die;
- the 4th heating scheme: heating the pressure die, wiper die, mandrel die and bend die, and without cooling the heat shields nearby the pressure die, wiper die and bend die;
- the 5th heating scheme: heating the pressure die, wiper die, mandrel die and part of the bend die (at the bend pointcut), and at the same time, cooling the heat shields nearby the pressure die, wiper die and bend die;
- the 6th scheme: heating pressure die, wiper die, mandrel die and part of the bend die (at the bend pointcut), and at the same time, cooling the heat shields nearby the pressure die and wiper die.

3.2 Evaluation of temperature distribution

The pressure die, mandrel die and wiper die are the main dies having important effects on temperature distribution especial nearby the point of contact. Therefore, the investigation of temperature distribution for the pressure die, mandrel die, wiper die and Ti–6Al–4V tube under different heating schemes is available to determine the proper heating method. The θ is the angle along the hoop direction of the Ti–6Al–4V tube (Fig. 11).

For the pressure die and wiper die, the temperature distributions on the ridge ($\theta = 180°$), the centerline ($\theta = 90°$) and the 45° position ($\theta = 135°$) of cavity surface

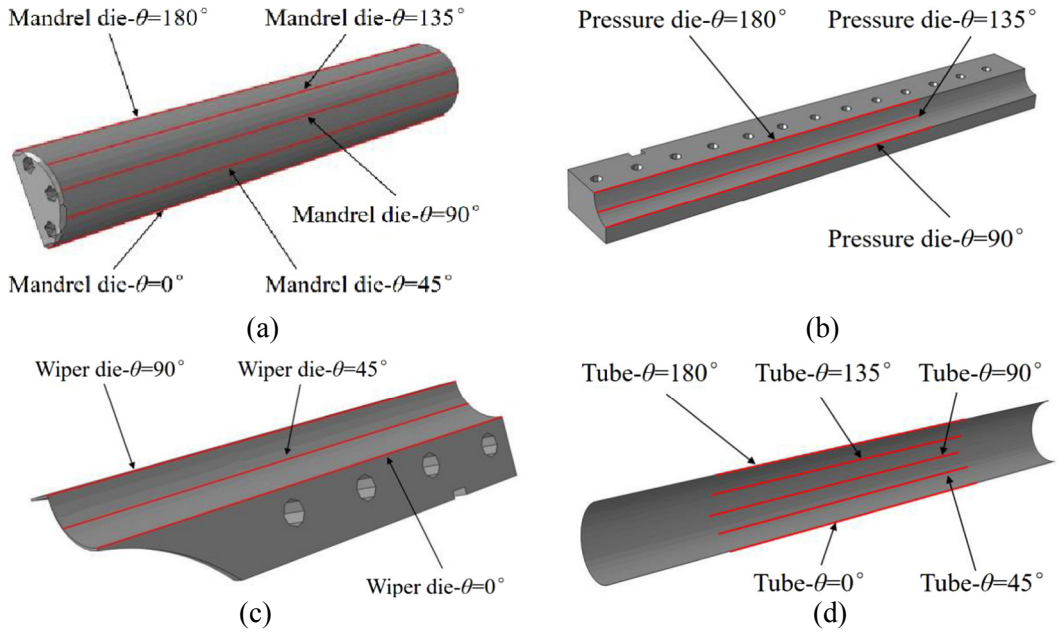

Fig. 12. Locations of temperature detection for different dies: (a) pressure die; (b) mandrel die; (c) wiper die; and (d) Ti–6Al–4V tube.

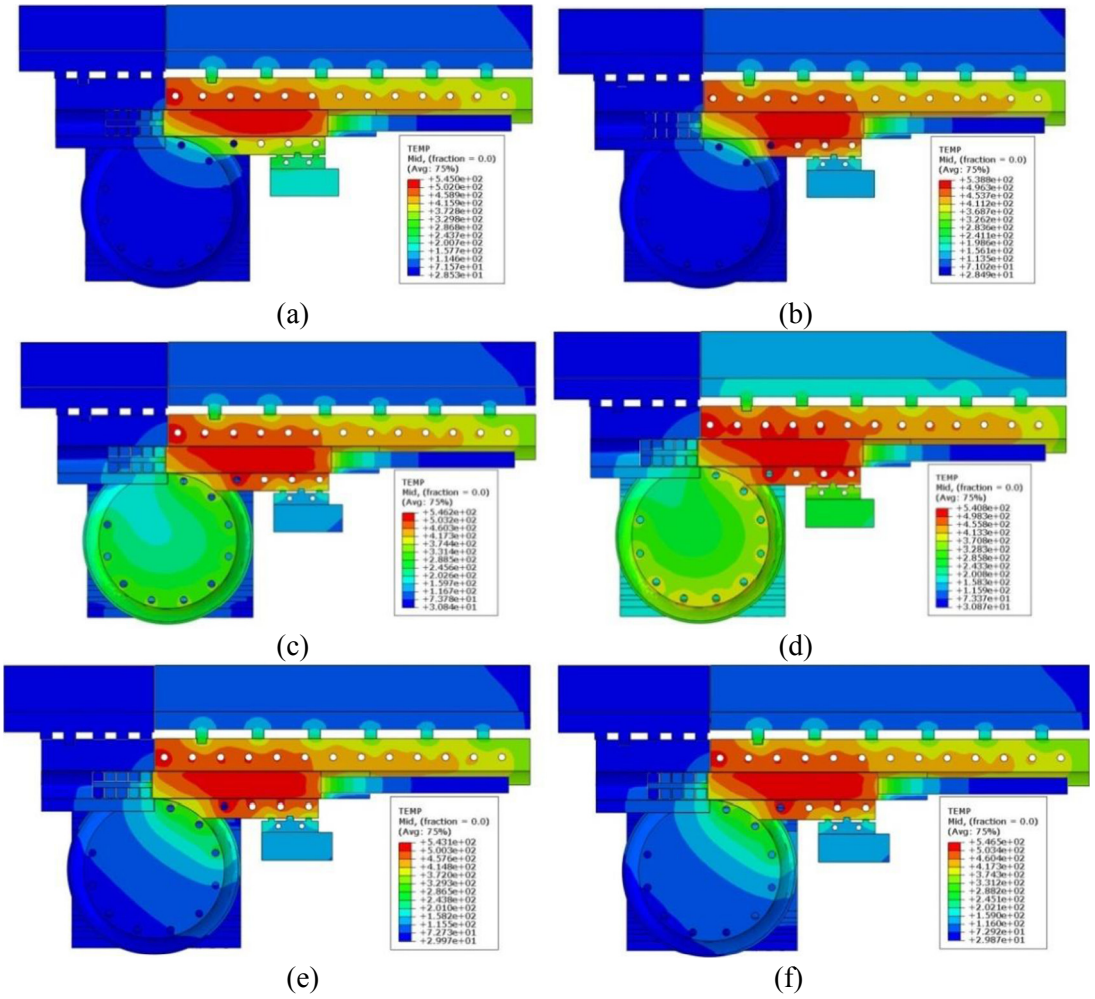

Fig. 13. The overall temperature distributions of heating model under different heating schemes: (a) 1st heating scheme; (b) 2nd heating scheme; (c) 3rd heating scheme; (d) 4th heating scheme; (e) 5th heating scheme; and (f) 6th heating scheme.

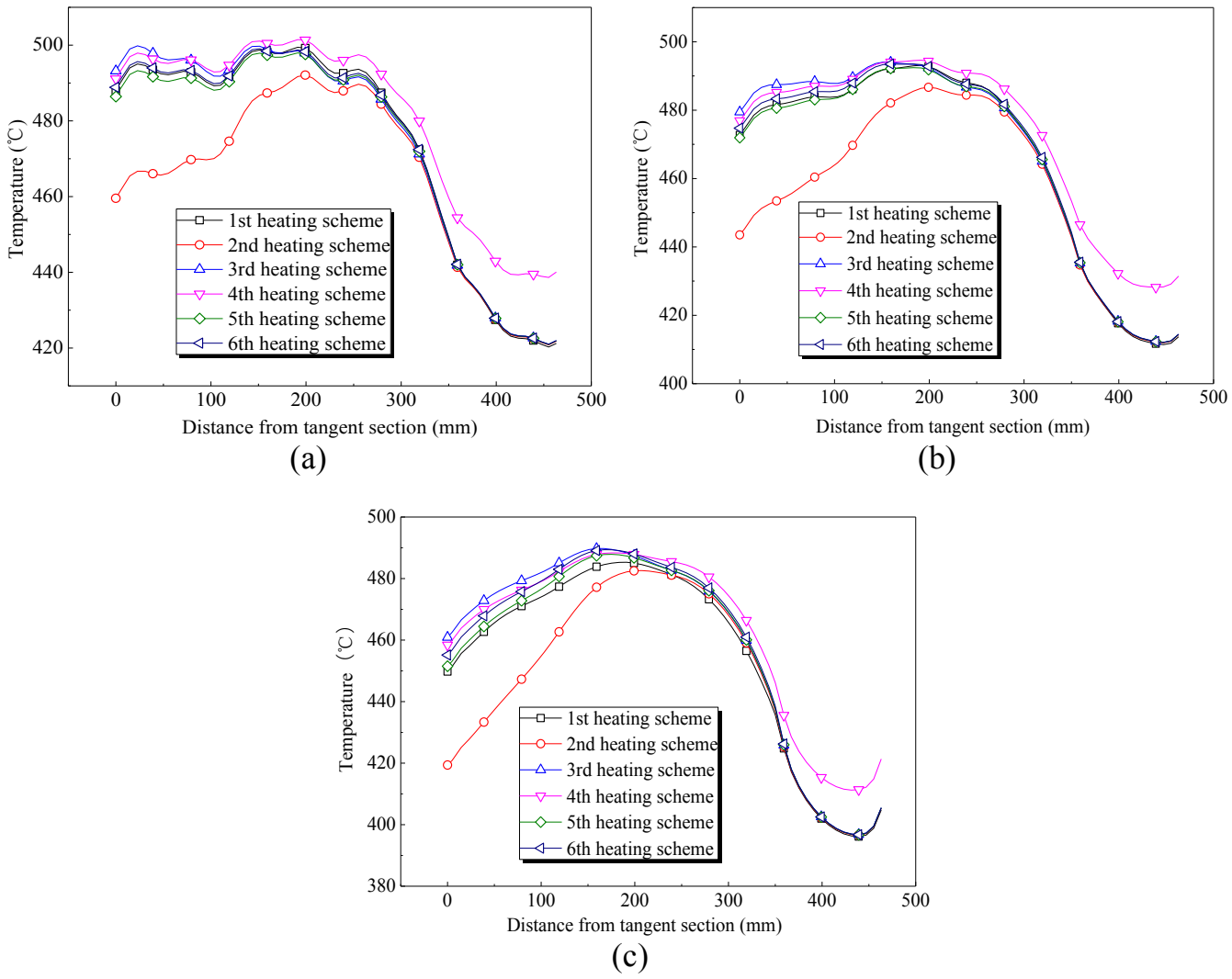

Fig. 14. The temperature distribution of different locations on pressure die under different heating schemes: (a) pressure die-$\theta = 180°$; (b) pressure die-$\theta = 135°$; and (c) pressure die-$\theta = 90°$.

are mainly investigated, shown as Figure 12a and c. For mandrel die and Ti–6Al–4V tube, the temperature distributions on the ridges ($\theta = 0°$ and 180°), the centerline ($\theta = 90°$) and the 45° position ($\theta = 45°$ and 135°) of cavity surface are mainly investigated, shown as Figure 12b and d.

3.3 Temperature distribution of different heating schemes

3.3.1 Overall temperature distribution

Based on the established model of heating stage, the six heating schemes as described above are simulated. The heating positions and thermometer holes are in line with the actual dies. The heating rods placed in mandrel die have the individual heating power of 800 W, and others have 600 W for each. Considering the ideal elongation of Ti–6Al–4V will be achieved at 500 °C, this temperature is set as the target temperature. The heating time is set as 4800 s to ensure sufficient heat transfer between the tube and dies. Figure 13 shows the overall temperature distribution under different heating schemes. From Figure 13a and b, serious heat consumption of bend die makes the temperature on wiper die and the front end of mandrel die much lower than the target temperature. Seen from Figure 13c and d, the application of cooling equipment prevents the heat transfer between dies and bending machine obviously with little effect on the temperature distribution on the bend die. Without the protection from cooling system, the temperature of bending machine will arrive upon 200 °C leading to the decrease of stability. However, the temperature of bending machine can be controlled under 100 °C with the use of cooling system. Shown as Figure 13e and f, whether be cooled or not, the bend die will not affect the overall temperature distribution when the bend die is heated partly. Meanwhile, whether the bend die be heated partly or not, the overall temperature distribution will be little influenced.

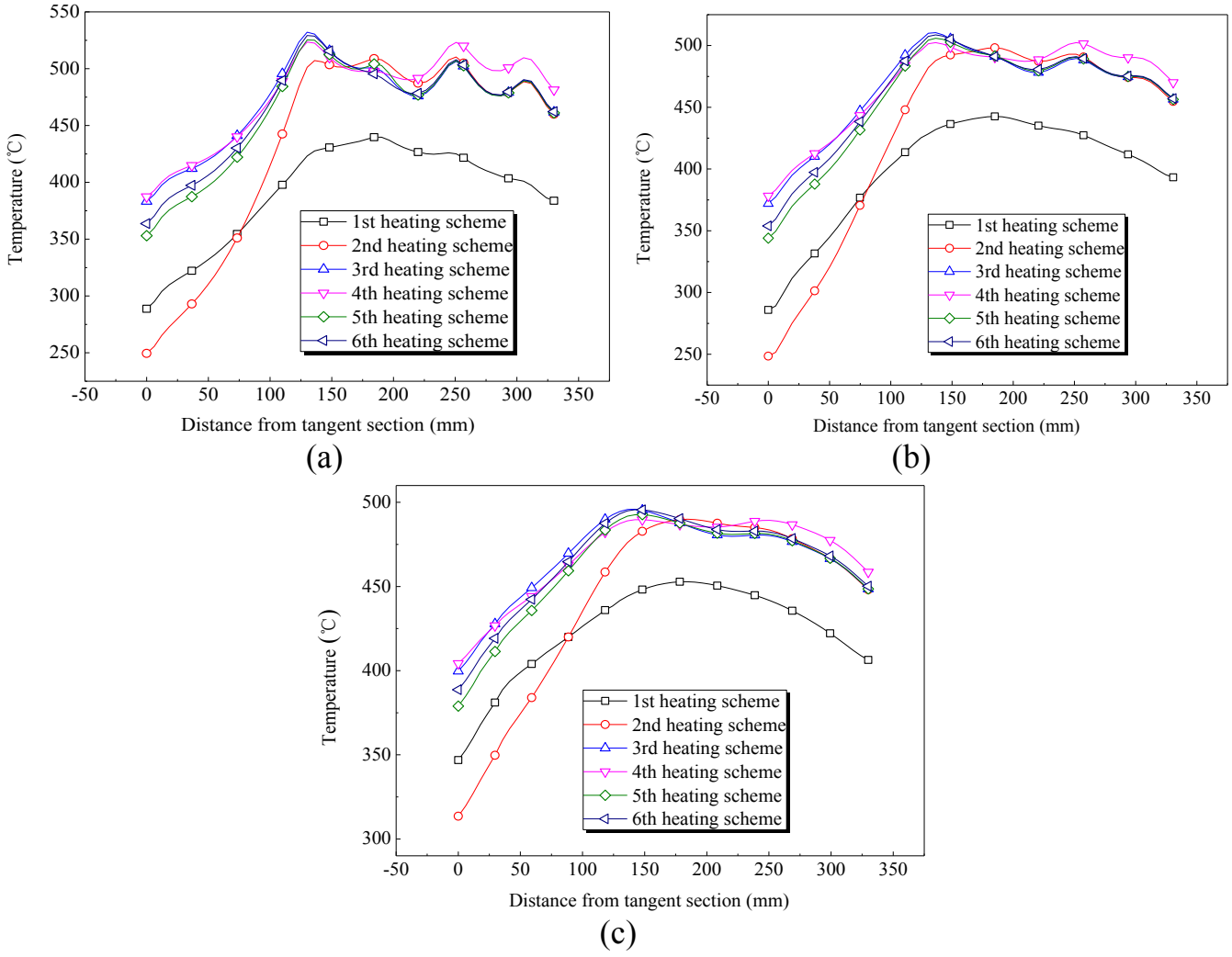

Fig. 15. Temperature distribution of different locations on wiper die under different heating schemes: (a) wiper die-$\theta = 90°$; (b) wiper die-$\theta = 45°$; (c) wiper die-$\theta = 0°$.

3.3.2 Comparison of heating effects on pressure die and wiper die

Figure 14 shows the temperature distribution of different locations on pressure die under different heating schemes. The axial temperature distribution on the pressure die is almost the same except being heated by the 2nd scheme. In the 2nd scheme, the front end of pressure die has lower temperature. Because the size constraints of wiper die, the heating holes only can be located far away from the bend die, which makes the back end of mandrel reach the desired temperature easily. However, the front end of mandrel die will transfer heat to bend die, which will decrease the overall temperature. Comparing the 3rd and 4th schemes, the temperature on pressure die will decrease about 20 °C when the cooling system is applied between bend die and bending machine. When heating according to the scheme of 3rd, 4th, 5th and 6th, the temperature distribution on the front end of pressure die has no significant change. At the same time, due to the combined effects of the radiation cooling, water cooling and air convection, the target temperature of 500 °C will not be achieved by heating the pressure die alone with the current heating power. As a result, an overall coordination on heating the different dies is necessary.

It is difficult to achieve the target temperature on bending pointcut under 1st and 2nd heating scheme (Fig. 15). There is no significant difference between temperature distribution on the wiper die under 3rd and 4th scheme. Compared with the 3rd scheme, the temperature achieved by the 5th scheme is 30 °C lower and by the 6th one is 20 °C lower. Therefore, for the wiper die, heating on the bend die locally can achieve the same effect compared with heating on the whole bend die.

3.3.3 Contrast of heating effects on mandrel and Ti–6Al–4V tube

Figure 16 shows the temperature distribution of different locations on the mandrel die under different heating schemes. Because of the cooling effect of bend die, the temperature on the front end of the mandrel is lower than the back end. From comparing Figure 16a and b, there is no significant difference between the axial temperature

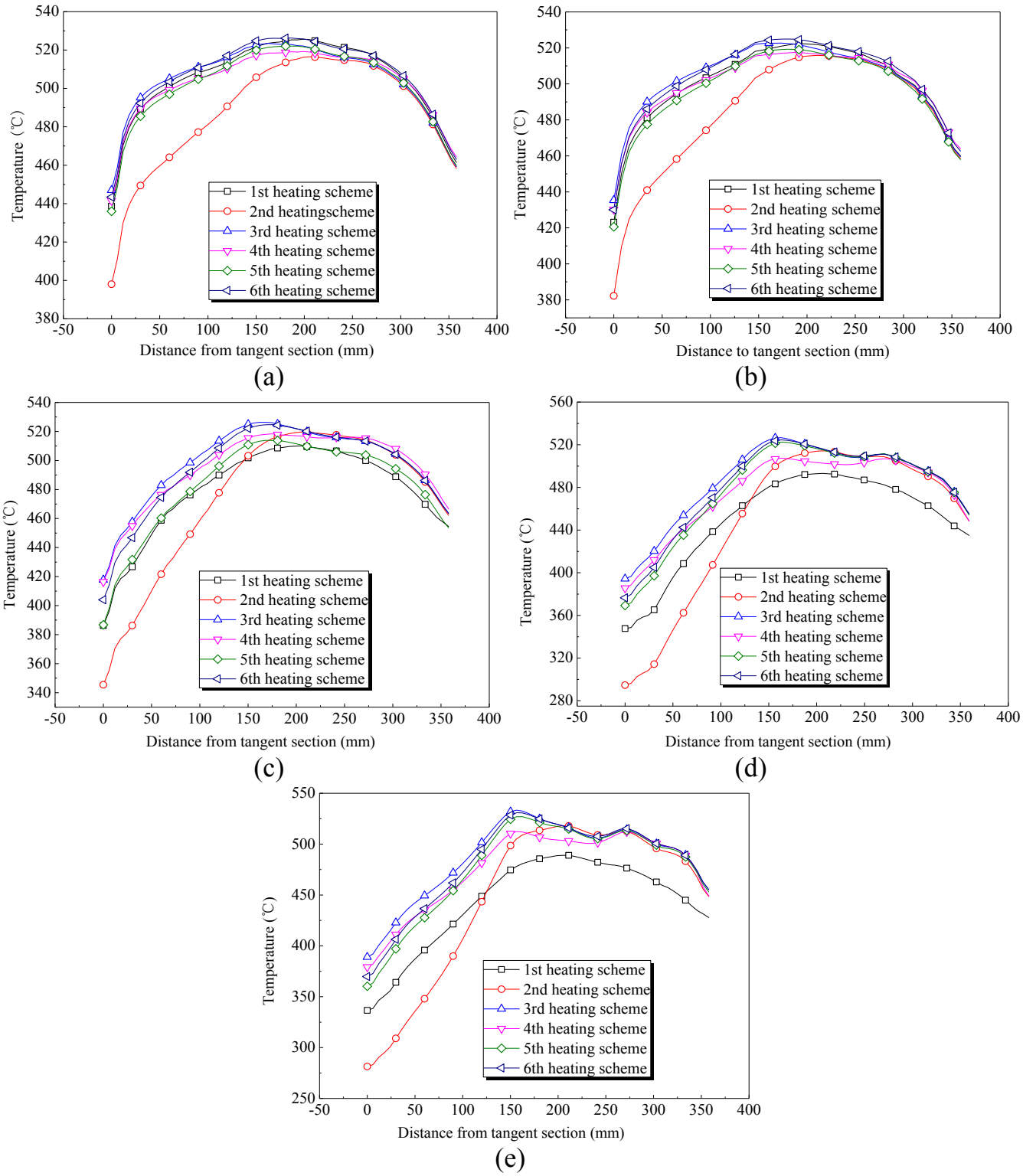

Fig. 16. Temperature distribution of different locations on mandrel die under different heating schemes: (a) mandrel die-$\theta = 180°$; (b) mandrel die-$\theta = 135°$; (c) mandrel die-$\theta = 90°$; (d) mandrel die-$\theta = 45°$; and (e) mandrel die-$\theta = 0°$.

distributions under different heating schemes except the 2nd scheme. As shown in Figure 16c–e, in the 2nd scheme, the temperature on the front end of the mandrel is much lower than that on the back end of the mandrel, which is similar to other heating schemes. Owing to the different combination of heating and cooling, the temperature on the front end of the mandrel has slight difference under the 3rd–6th schemes. The temperature on the inner front end achieved by the 5th scheme is 50 °C lower than that achieved by the 3rd scheme. Without cooling system, the

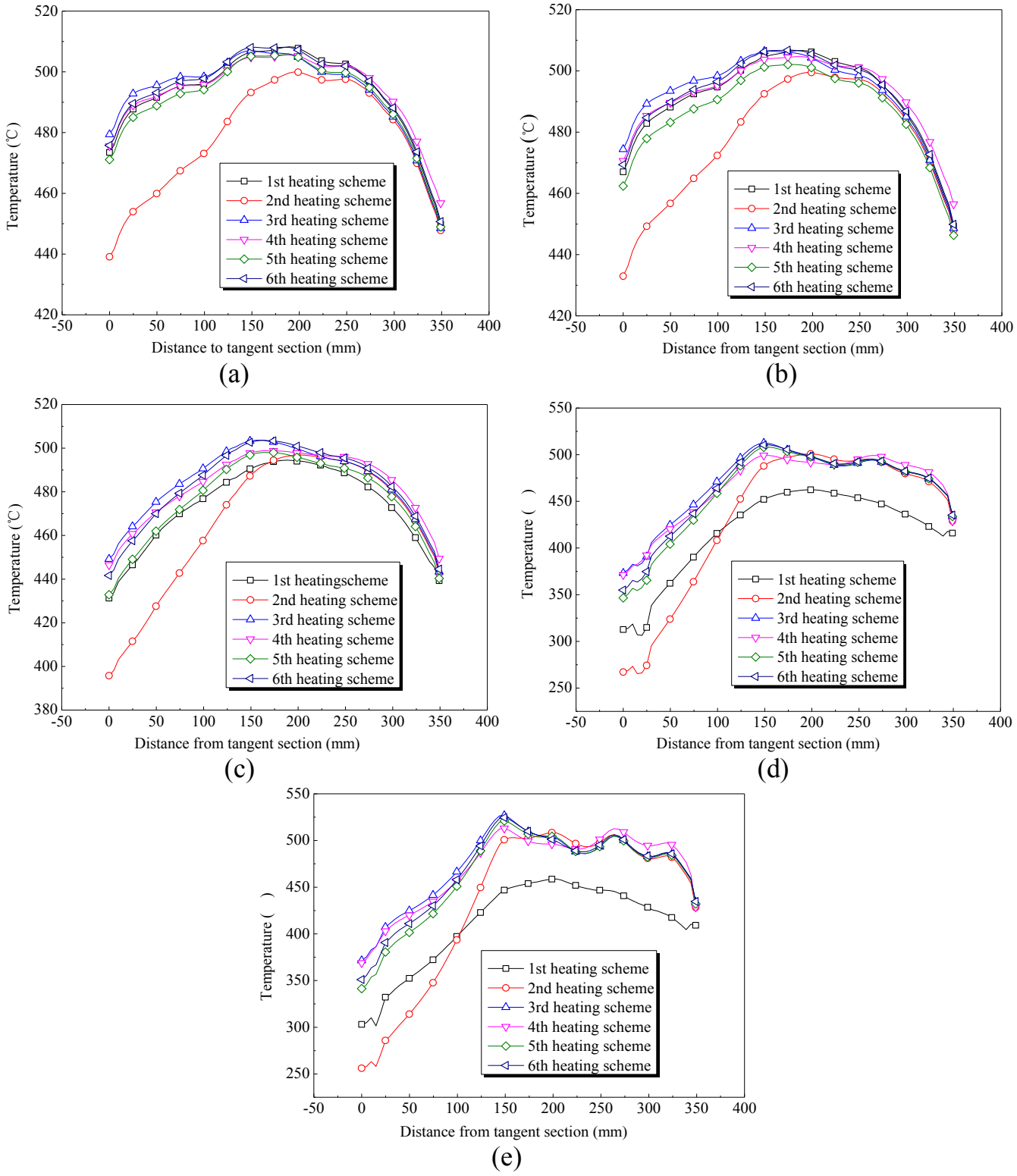

Fig. 17. Temperature distribution of different locations on Ti–6Al–4V tube under different heating schemes: (a) tube-$\theta = 180°$; (b) tube-$\theta = 135°$; (c) tube-$\theta = 90°$; (d) tube-$\theta = 45°$; and (e) tube-$\theta = 0°$.

temperature difference is about 20 °C comparing the 3rd and 6th scheme. Therefore, for the mandrel die, heating on the bend die locally can achieve the same effect compared with heating on the whole bend die.

The temperature distribution rule of the different locations on the Ti–6Al–4V tube under different heating schemes is shown in Figure 17, which is similar to the temperature distribution rule of the mandrel die.

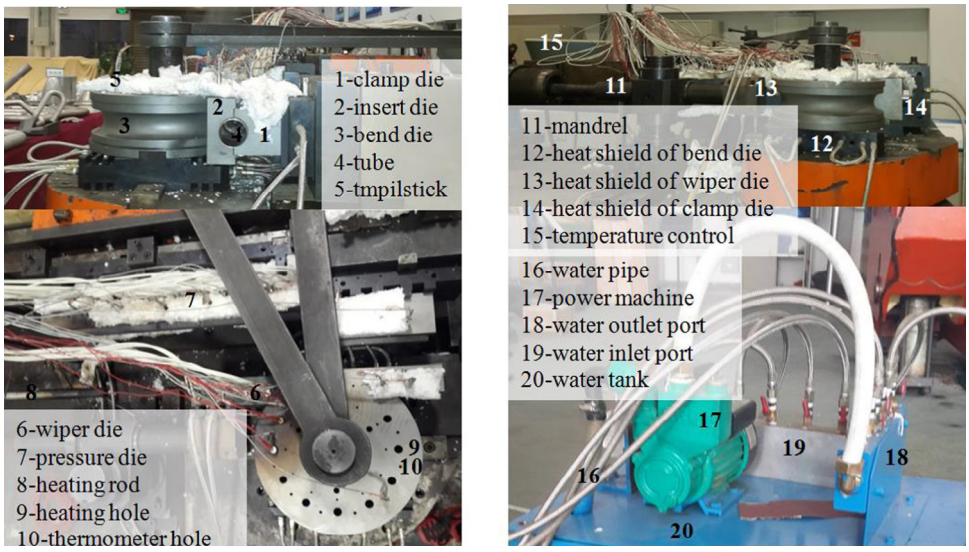

Fig. 18. Assembly of warm bending dies seen from top view (a) and cooling system fitted to W27YPC-159 bending machine (b).

Considering Figure 17a and b, the 1st and 2nd schemes are ruled out. In the 3rd and 4th schemes, all of the heating holes are used leading to 20 °C higher temperature than heating bend die partly (in the 5th and 6th schemes). Therefore, the front end of Ti–6Al–4V tube has higher temperature because of the hotter bend die.

3.4 Optimal selecting of heating scheme

Based on the comprehensive analysis of the temperature distribution on the tube and dies, increasing the heating power is difficult to make the front end of Ti–6Al–4V tube reach the target temperature due to the large heat loss of heat transfer in the contact area between the bend die and bending machine. From the influence of temperature distribution on tube forming quality, the low temperature of the inside was beneficial to the improvement of the forming quality. Therefore, there is no need to increase the heating power deliberately in pursuit of uniform temperature distribution on the inside and outside of tube. Comparing the heating effect of different heating schemes, from the 3rd to 6th schemes, a higher temperature can be achieved on the inside of the tube, and the temperature can be controlled widely. Considering the heating efficiency, although the 3rd and 4th schemes can reach 20 °C higher temperature than the 5th and 6th ones, a disadvantage of high energy consumption makes the bend die no need to be heated wholly. In the 5th scheme, the cooling system takes away part of heat and ensures the insulation. However, the bend die is heated partly with no impossible to make the bending machine reach higher than 100 °C, which has slight effect on the running accuracy.

As a result, from the multi-factor comprehensively considering of heating efficiency, machine running accuracy and energy conservation, the 6th heating scheme is the optimal choice for the Ti–6Al–4V tube warm-bending. This scheme is specifically included heating the pressure die, mandrel die and wiper die wholly, heating the bend die partly (the location nearby wiper die), and cooling the pressure die and wiper die.

4 Application of the 3D FE model

Based on the FE model and lots of cool bending experiments, the dies have been manufactured and fitted to W27YPC-159 bending machine (Fig. 18), and the warm-bending experiments have been carried on successfully. Figure 19 shows the simulated results of Ti–6Al–4V LDTW tube after NC warm-bending. The simulation results shown in Figure 19a–c indicate that higher temperature brings about better deformation quality, which is in agreement with the material tensile tests. Then, the NC warm bending experiments under same conditions were carried out to compare with the simulation results, as shown in Figure 20a and b. As a result, the defects of over-thinning, wrinkling and fracture are predictable and the formation conditions of different kinds of defects can be well explained. The obtained results are very instructive for bending parameter optimization and process design. Through analyzing the warm-bending experiments, it is found that the formability of Ti–6Al–4V tube is improved by means of the elevated temperature. Other defects in real warm-bending experiments such as serious cross-section distortion and crack of the joint are shown in Figure 20c and d. Therefore, the 3D FE model of warm-bending, a three-stage process of heating-bending-unloading, is applied to simulate the warm-bending process under different process parameters and finally determine the appropriate parameters to achieve the qualified bent tube. The simulation reduces the number of trial and error tests, saves the test materials and energy consumption, and avoids the wear away of dies and heating equipment.

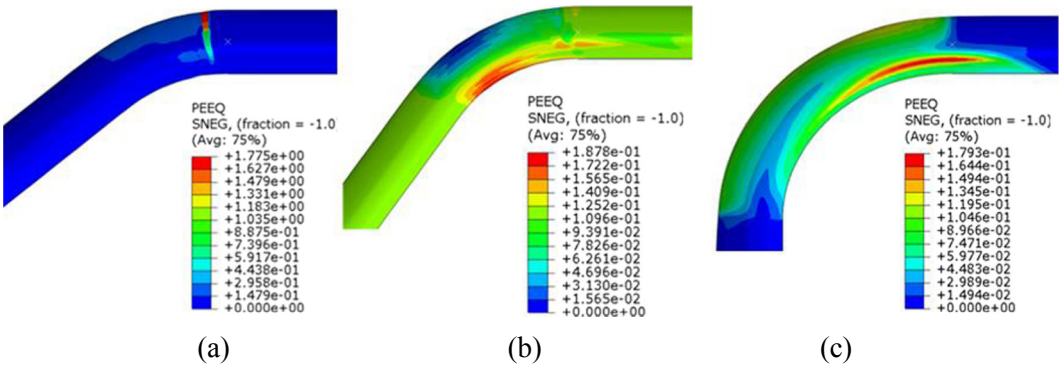

Fig. 19. Defects in simulated warm-bending results of LDTW Ti–6Al–4V tube: (a) simulated fracture, (b) simulated wrinkling, and (c) simulated preferable result.

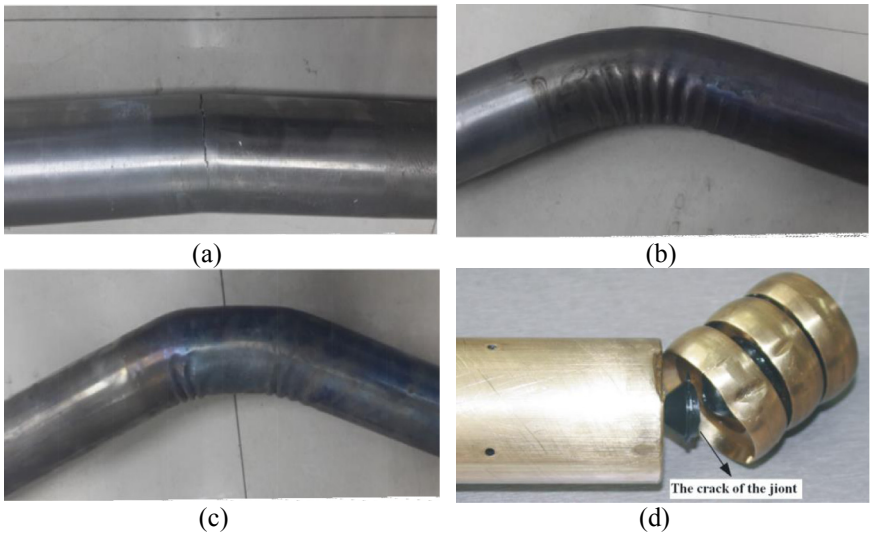

Fig. 20. Defects in experimental warm-bending results of LDTW Ti–6Al–4V tube: (a) fracture; (b) wrinkling; (c) cross-section distortion; and (d) crack of the joint.

Fig. 21. Qualified 90° bent tube made by warm bending: (a) top view and (b) side view.

Excellent bent tube (Fig. 21) has been achieved based on extensive simulation and experiment. To sum up, the established heating-bending-unloading model is reliable.

5 Conclusions

In this study, thermal-mechanical coupled FE model for warm-bending of LDTW Ti–6Al–4V tube has been established and used to simulate the complete warm-bending process. The conclusions can be drawn as following:

- based on ABAQUS, the three-stage model of heating-bending-unloading is developed considering the characteristics of multi-die constraints and local heating. In this model, various parameters such as geometry sizes, material properties and load-curve, are determined based on the actual experiment in terms of both accuracy and efficiency;
- six combination schemes of heating system in heating stage of warm-bending are given and compared according to comprehensive consideration of heating efficiency, machine running accuracy and energy conservation. The optimal selecting is the 6th one, which is specifically included heating on the pressure die, mandrel die and wiper die wholly, and heating on the bend die partly (the location nearby wiper die) as well as cooling to the pressure die and wiper die;
- through large amounts of simulations and experiments, there is abundant evidence showing that the thermal–mechanical coupled FE model can be helpful as a replacement or supplementary to physical experiment. The FE simulation allows process analysis to be performed at a lower cost with giving a better understanding of deformation predictions for warm-bending of LDTW Ti–6Al–4V tube.

The authors thank the National Science Fund for Excellent Young Scholars (51522509), the National Natural Science Foundation of China (51275415), the Research Fund of the State Key Laboratory of Solidification Processing (NWPU) (KP201608) and the EU Marie Curie Actions – MatProFuture Project (FP7-PEOPLE-2012-IRSES-318968). Especially, the authors want to extend the heartfelt gratitude to our supervisor, Professor He Yang, whose patient guidance, valuable suggestions and constant encouragement make us successfully complete this thesis.

References

[1] H. Yang et al., Chin. J. Aeronaut. 25 (2012) 1–12
[2] M.S.J. Hashmi, J. Mater. Process. Technol. 179 (2006) 5–10
[3] H. Li et al., Int. J. Plast. 90 (2017) 177–211
[4] G.G. Yapici, I. Karaman, Z.P. Luo, Acta Mater. 54 (2006) 3755–3771
[5] R.R. Boyer, Mater. Sci. Eng. A 213 (1996) 103–114
[6] H. Li et al., J. Mater. Process. Technol. 212 (2012) 1973–1987
[7] J.D. Beal, R. Boyer, D. Sanders, ASM handbook, volume 14: metalworking: sheet forming, ASM International, 2006, pp. 656–669
[8] X. Li et al., Mater. Des. 55 (2014) 325–334
[9] Z.J. Tao et al., Chin. J. Aeronaut. 29 (2016) 542–553
[10] Z.J. Tao et al., Rare Metals 35 (2016) 162–171
[11] N. Kotkunde et al., Mater. Des. 63 (2014) 336–344
[12] C.P. Lai, L.C. Chan, C.L. Chow, J. Mater. Process. Technol. 191 (2007) 157–160
[13] G. Chen et al., Mater. Des. 83 (2015) 598–610
[14] W.Y. Wu et al., Mater. Sci. Eng. A 486 (2008) 596–601
[15] A.A. Luo, A.K. Sachdev, Mater. Sci. Forum 488–489 (2005) 477–482
[16] L. Jin et al., J. Mater. Sci. 47 (2012) 3801–3807
[17] Z.Y. Zhang et al., Mater. Sci. Eng. A 569 (2013) 96–105
[18] V. Romanova et al., Comput. Mater. Sci. 28 (2003) 518–528
[19] U. Weber et al., Comput. Mater. Sci. 32 (2005) 577–587
[20] H. Grass, C. Krempaszky, E. Werner, Comput. Mater. Sci. 36 (2006) 480–489
[21] N. Bontcheva, G. Petzov, Comput. Mater. Sci. 34 (2005) 377–388
[22] H. Grass et al., Comput. Mater. Sci. 28 (2003) 469–477
[23] J.L. Feng, Y. Qin, H.S. Dong, Manuf. Rev. 3 (2016) 6
[24] J. Liu et al., Manuf. Rev. 3 (2016) 8
[25] H. Li, H. Yang, M. Zhan, Modell. Simul. Mater. Sci. Eng. 17 (2009) 35007–35039
[26] R.J. Gu et al., Comput. Mater. Sci. 42 (2008) 537–549
[27] H. Yang et al., Comput. Mater. Sci. 45 (2009) 1052–1067
[28] H. Li et al., Comput. Mater. Sci. 45 (2009) 921–934
[29] C. Li et al., Trans. Nonferrous Metals Soc. China 19 (2009) 668–673
[30] Z.Q. Jiang et al., Int. J. Mech. Sci. 52 (2010) 1115–1124
[31] Z.Q. Jiang et al., Mater. Des. 31 (2010) 2001–2010
[32] K. Trana, J. Mater. Process. Technol. 127 (2002) 401–408
[33] Z.Y. Zhang et al., Int. J. Adv. Manuf. Technol. 72 (2014) 1187–1203
[34] Z. Hu, J.Q. Li, J. Mater. Process. Technol. 91 (1999) 75–79
[35] Z. Hu. J. Mater. Process. Technol. 102 (2000) 103–108
[36] W. Zhou, L. Zhou, Z.T. Yu, Rare Metal Mater. Eng. 34 (2005) 1585–1587 (in Chinese)
[37] L.T. Li et al., Forg. Stamp. Technol. 31 (2006) 131–134 (in Chinese)
[38] Y. Dai et al., Rare Metal Mater. Eng. 38 (2009) 1801–1806 (in Chinese)
[39] Z.J. Tao et al., Trans. Nonferrous Metals Soc. China, in press
[40] J. Ma et al., Trans. Nonferrous Metals Soc. China 25 (2015) 2924–2931
[41] D. Wang et al., Chin. J. Aeronaut. 27 (2014) 1002–1009

Cite this article as: Zhijun Tao, Heng Li, Jun Ma, Heng Yang, Chao Lei, Guangjun Li, FE modeling of a complete warm-bending process for optimal design of heating stages for the forming of large-diameter thin-walled Ti–6Al–4V tubes, Manufacturing Rev. **4**, 8 (2017)